35th Annual International Conference of the IEEE EMBS
Osaka, Japan, 3 - 7 July, 2013

Electrical Morris-Lecar neuron

Rachid Behdad [1], Stéphane Binczak [1], Vladimir I. Nekorkin [2],
Alexey S. Dmitrichev [2] and Jean-Marie Bilbault [1]

***Abstract*— In this study, an experimental electronic neuron based on Morris-Lecar model is presented, able to become an experimental unit tool to study collective association of robust coupled neurons. The circuit design is given according to the ionic currents of this model. The experimental results are compared to the theoretical prediction, leading to validate this circuit.**

I. INTRODUCTION

A key problem to study brain behavior is to understand how the neurons represent and bind sensory information converging to the brain from different channels. Neurons exhibit and transmit electrical activity that researchers try to model by different ways. While the most famous model has been developed by Hodgkin and Huxley (HH) [1], some of its derived models, as FitzHugh Nagumo (FHN) [2], [3] or Morris-Lecar (ML) [4], [5], [6] ones, despite their simplicity, give interesting results as different behaviors appear according to tunable parameters. Nowadays, computer simulation of large scale neural is more powerful, but they are rarely able to work in real time, as the number of equations to be solved can be important. When using analog electronic circuits, the real-time calculation is possible. If these circuits work in real time, we obtain an artificial neuron able to reproduce the behavior of a real neuron [7], [8]. It is easy to further accelerate the analog simulator performance by dividing by given factor all kinetic parameters.

In the present work, we propose a complete electronic implementation of ML model of type I, candidate to become an experimental unit tool to study collective association of robust coupled neurons. Experiments on this electrical neuron can enlighten the robustness of the obtained behaviors as it includes intrinsic and extrinsic noise. We present firstly the equation set of ML model, then the circuit design. Finally, we compare our experimental results with the various theoretical predictions of this model.

II. THE MORRIS-LECAR MODEL

The Morris-Lecar model [4] of biological neuron was developed to reproduce the variety of oscillatory behaviors with respect to the calcium Ca^{++} and potassium K^{+} conductances in the giant barnacle muscle fiber. The Morris-Lecar model is a two-dimensional system of nonlinear differential equations:

$$C_m \frac{dV}{dt} = -g_{Ca} M_\infty(V) \cdot (V - V_{Ca}) - g_K W \cdot (V - V_K) - g_L (V - V_L) + I_{app}, \tag{1a}$$

$$\frac{dW}{dt} = \frac{W_\infty(V) - W}{\tau_W(V)}, \tag{1b}$$

where

$$M_\infty(V) = \frac{1}{2} + \frac{1}{2} \tanh\left(\frac{V - V_1}{V_2}\right) \tag{2}$$

$$W_\infty(V) = \frac{1}{2} + \frac{1}{2} \tanh\left(\frac{V - V_3}{V_4}\right) \tag{3}$$

$$\tau_W(V) = \frac{T_0}{\cosh\left(\frac{V - V_3}{2V_4}\right)} \tag{4}$$

V is the membrane voltage, C_m is the membrane capacitance and I_{app} is the current applied to the neuron. $I_{Ca} = g_{Ca} M_\infty(V).(V - V_{Ca})$, $I_K = g_K W.(V - V_K)$ and $I_L = g_L(V - V_L)$ are the calcium, potassium and leak currents respectively in $\mu A/cm^2$, wherein W represents the recovery variable. The calcium Ca^{++} activates the membrane and the potassium K^{+} depolarizes this membrane. g_{Ca}, g_K and g_L are conductances for Ca^{++}, K^{+}, and $leak$ ion channel respectively. V_{Ca}, V_K and V_L are equilibrium potentials corresponding to the currents. V_1, V_2, V_3 and V_4 are setting parameters for steady states. The values of the different parameters of type I are listed in Table I [6]. This model presents both neurons Class I and Class II. Class I neurons begin repetitive discharges with a frequency close to zero. On the other hand, class II neurons begin repetitive discharges with a finite frequency.

To generate a response, the membrane must be excited above a certain threshold. Below this threshold, the neuron rapidly returns to its equilibrium position. On the other hand, if the excitation exceeds the threshold, then the neuron sends a response to this stimulation as a train of some oscillations. The Morris-Lecar model shows the relationship that links membrane voltage and activation of ion channels.

III. ELECTRONIC CIRCUIT

To simplify the design of the circuit, we decompose it into several parts (ionic currents) and realize each part with

[1]R. Behdad, S. Binczak and J. M. Bilbault are with the Laboratoire LE2I CNRS UMR 6306, Université de Bourgogne, 9 avenue Alain Savary, 21078 Dijon, France.

[2]V. I. Nekorkin and A. S. Dmitrichev are with the Institute of Applied Physics of RAS, 603950, 46 Ulyanova Str., Nizhny Novgorod, Russia.

TABLE I

FIXED PARAMETERS FOR THE M-L MODEL[6]

Parameter	Value	Parameter	Value
C_m	20 ($\mu F/cm^2$)	g_{Ca}	4 (mS/cm^2)
g_K	8 (mS/cm^2)	T_0	15 (ms)
g_L	2 (mS/cm^2)	V_1	- 1.2 (mV)
V_{Ca}	120 (mV)	V_2	- 18 (mV)
V_K	- 80 (mV)	V_3	12 (mV)
V_L	- 60 (mV)	V_4	17.4 (mV)

discrete and active components (see Fig. 1) according to:

$$C_m \frac{dV}{dt} = -I_{Ca} - I_K - I_L + I_{app} \tag{5}$$

where

$$I_{Ca} = g_{Ca} M\infty(V) \cdot (V - V_{Ca})$$
$$I_K = g_K W (V - V_K)$$
$$I_L = g_L (V - V_L)$$

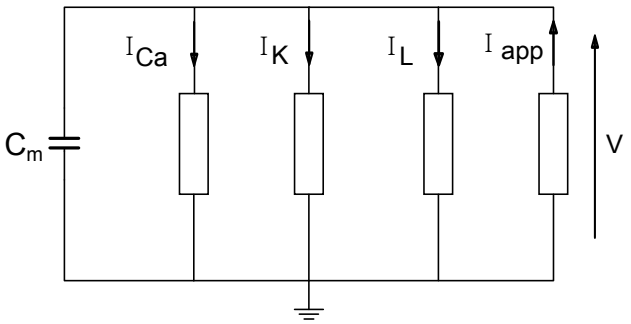

Fig. 1. Equivalent circuit for the M-L model

A. The calcium current

To build the current I_{Ca} (see block A, Fig. 4), we use 2 Operational Transconductance Amplifiers (OTA) LM13700 [9], whose gain can be controlled via either bias current or diode current. To obtain the slope of the sigmoid function $M_\infty(V)$ according to eq (2), we amplify a OTA 1 entry tension with an operational amplifier (OA) UA741. With the OTA 2, we multiply both signals $g_{Ca} M_\infty(V)$ and $(V - V_{Ca})$. Fig 2(a) shows comparison of experimental and theoretical results of the calcium current I_{Ca}.

B. The potassium current I_K

To solve the problem of the differential equation (1b) we build a circuit with a capacitance C_1 and a nonlinear resistance Rnl (see Fig 3).

From this circuit we can write:

$$C_1 \frac{dW}{dt} = I_a - I_b = I_a - \frac{W}{Rnl}$$
$$\frac{dW}{dt} = \frac{1}{C_1}\left(I_a - \frac{W}{Rnl}\right) = \frac{1}{C_1 Rnl}\left(I_a \cdot Rnl - W\right)$$

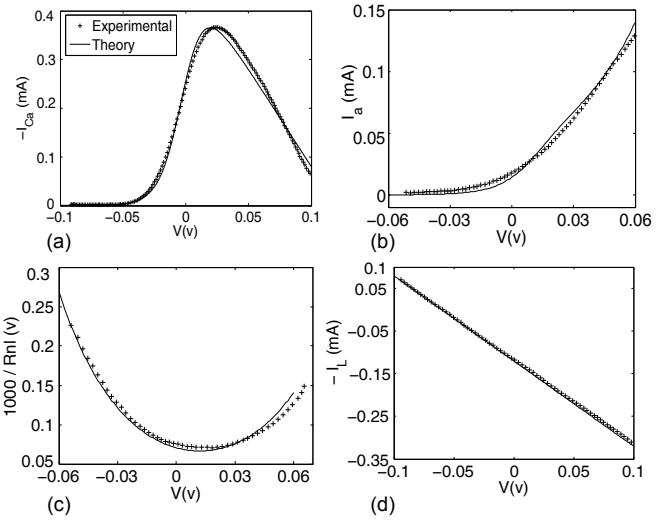

Fig. 2. (a), (b) and (d) shows comparison of experimental (solid line) and theoretical (+) results of I_{Ca}, I_a and $leak$ current respectively. (c) shows the catenary cuve.

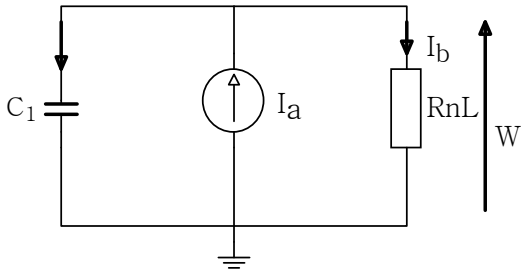

Fig. 3. Capacitance C_1 and a nonlinear resistance (Rnl)

$$\Rightarrow \begin{cases} \tau_W(V) = C_1 Rnl \\ W_\infty(V) = I_a \cdot Rnl \end{cases} \Rightarrow \begin{cases} Rnl = \dfrac{\tau_W(V)}{C_1} \\ I_a = \dfrac{W_\infty(V)}{Rnl} \end{cases}$$

$$\Rightarrow \begin{cases} Rnl = \dfrac{T_0}{C_1 \cosh\left(\frac{V - V_3}{2V_4}\right)} \\ I_a = \dfrac{C_1}{2T_0}\left[1 + \tanh\left(\dfrac{V - V_3}{V_4}\right)\right] cosh\left(\dfrac{V - V_3}{2V_4}\right) \end{cases} \tag{6}$$

From the previous circuit, we can write:

$$I_b = \frac{W}{Rnl}$$

We can notice that in block B_2 (see Fig. 4), the nonlinear resistance is function of the membrane voltage V. Now we build the different circuits giving I_a and I_b currents and the catenary voltage. We put: $C_1 = 1\mu F$.

1) Current I_a: it is given by block B_1 in Fig. 4, which is composed by an OTA, an OA and current sources. Fig 2(b) shows comparison of experimental and theoretical results of I_a current.

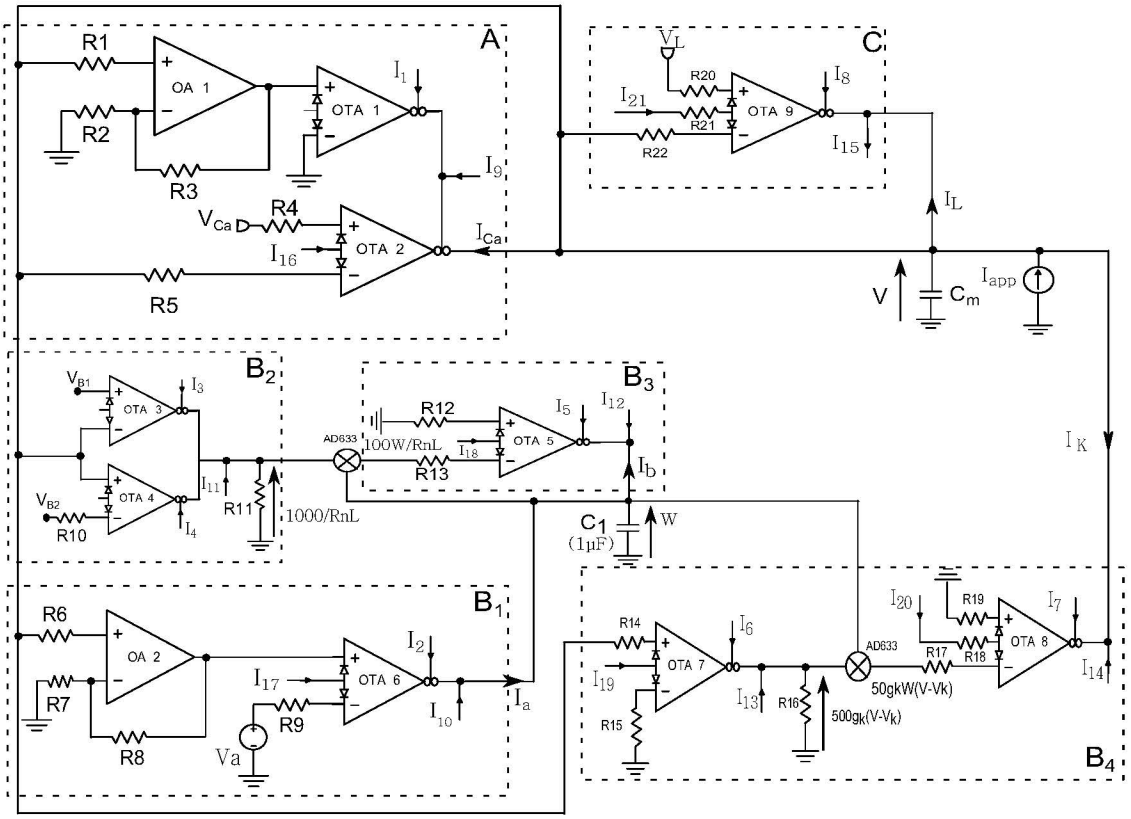

Fig. 4. Global circuit where I_1 to I_8 are bias currents, I_9 to I_{15} are offset currents and I_{16} to I_{21} are diode currents.

2) Catenary curve $1000/Rnl$*:* it is obtained by adding output currents of 2 OTAs, with inverted inputs, as shown in block B_2. Fig 2(c) shows comparison of experimental and theoretical results of catenary.

3) Current I_b*:* it is produced with an analog multiplier (AD633) and a voltage-current converter (see block B_3).

4) Current I_k*:* To complete the production of I_k current, we use an OTA for the voltage $500g_K(V - V_K)$ and a multiplier by W. Finally another OTA is used as a voltage-current converter and negative multiplier by (-50) as shown in block B_4 (see Fig. 4).

C. The leak current $I_L = g_L(V - V_L)$

Only one OTA, restricted to its linear zone, is enough to give I_L (see block C, Fig. 4). Fig 2(d) shows comparison of experimental and theoretical results of leak current.

IV. Test of the Global Electronic Circuit

To test the neuron circuit build sketched in Fig. 4, initial conditions V_{in} and W_{in} are required: we used the switcher MC14066BCP and reversers with OA, and compare these experimental results with numerical simulations of the complete model ML (using a 4^{th} order Runge-Kutta scheme). Fig. 5 shows the different areas of bifurcation of codimension 2 (C_m, I_{app}). With this circuit, we have managed to clearly distinguish between the different areas of bifurcation. Now, we give some examples of neuron behaviors. In region 1, there is a single equilibrium point, which is illustrated in Fig. 6, where (a), (b) and (c) correspond to the experimental results of membrane potential, recovery variable and phase plane respectively. Theoretical nullclines (dashed lines) are placed in (c), we compare the phase plane obtained with the numerical simulation which is shown in (c). Arrows indicate directions of trajectories. In region 9 of Fig. 5, we found a stable cycle, which leads to the behaviors of Fig. 7. Finally, in region 7 of Fig. 5, no cycles exist (see Fig. 8). We find different behaviors for other regions, but we do not draw the border that separates the region 4 and 5 because they are very thin.

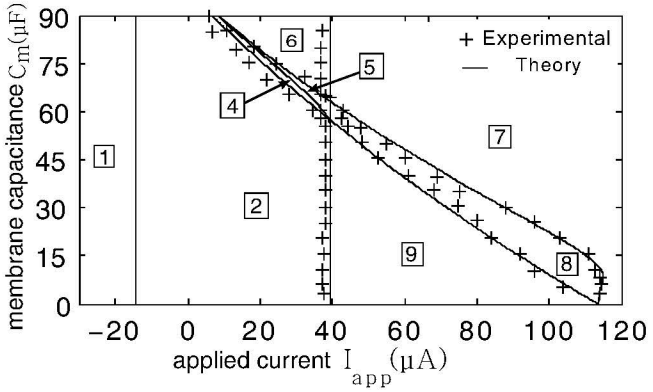

Fig. 5. bifurcation diagram of codimension 2 (C_m, I_{app})

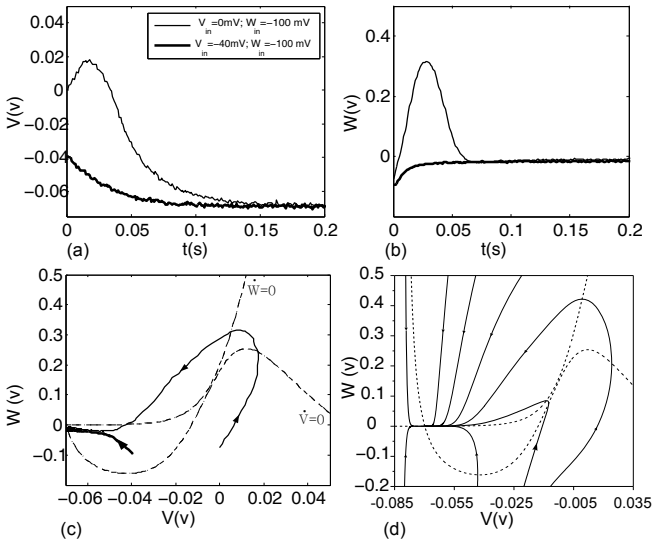

Fig. 6. region 1: $C_m = 60\mu F; I_{app} = -20\mu A$ with $V_{in} = -10mV$ and $W_{in} = -96mV$. (a): membrane potential versus time; (b): recovery variable versus time; (c): experimental phase plane and (d): theoretical phase plane.

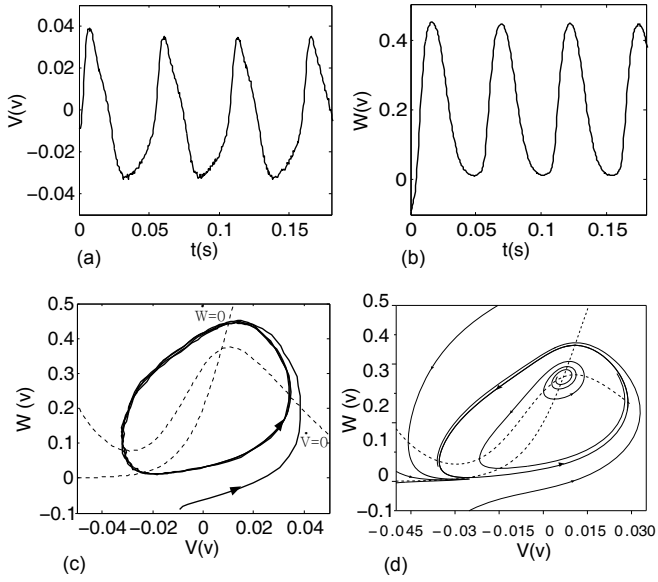

Fig. 7. region 9: $C_m = 20\mu F; I_{app} = 70\mu A$ with $V_{in} = -10mV$ and $W_{in} = -96mV$

V. Conclusion

It is worthwhile to remark that in our implementation of ML electronic neuron, $\tau_W(V)$ is indeed fonction of V according to Eq. (4) which improves the circuit given in [5]. Moreover, with OTA technology, switching to micro-electronics is easy. This circuit can become an experimental unit tool to study the robustness of collective dynamics of small size neuronal networks. The large-scale simulation of the neuron behaviors takes too much calculation time, but with electronic neurons, the real time results can be obtained. The next stage will be to couple a sufficient number of such neurons to obtain the Anti-phase spiking patterns in order

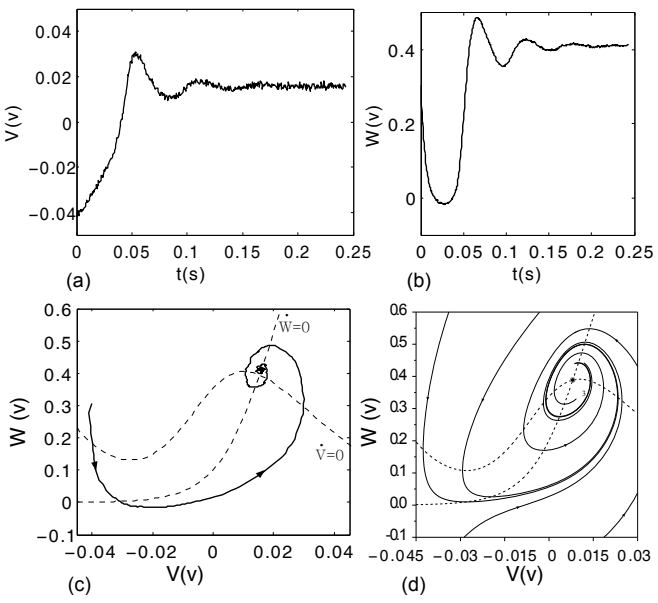

Fig. 8. region 7: $C_m = 60\mu F; I_{app} = 90\mu A$ with $V_{in} = -40mV$ and $W_{in} = 300mV$

to understand the anti-phase synchronization in biological systems.

References

[1] A. Hodgkin and A. Huxley, "A quantitative description of membrane current and its application to conduction and excitation in nerve," *The Journal of physiology*, vol. 117, no. 4, p. 500, 1952.

[2] R. Fitzhugh, "Impulses and physiological states in theoretical models of nerve membrane," *Biophysical journal*, vol. 1, no. 6, pp. 445–466, 1961.

[3] V. Kazantsev, A. Tchakoutio Nguetcho, S. Jacquir, S. Binczak, and J. Bilbault, "Active spike transmission in the neuron model with a winding threshold manifold," *Neurocomputing*, 2012.

[4] C. Morris and H. Lecar, "Voltage oscillations in the barnacle giant muscle fiber," *Biophysical journal*, vol. 35, no. 1, pp. 193–213, 1981.

[5] A. Wagemakers, M. Sanjuán, J. Casado, and K. Aihara, "Building electronic bursters with the Morris–Lecar neuron model," *International Journal of Bifurcation and Chaos*, vol. 16, no. 12, pp. 3617–3630, 2006.

[6] K. Tsumoto, H. Kitajima, T. Yoshinaga, K. Aihara, and H. Kawakami, "Bifurcations in Morris–Lecar neuron model," *Neurocomputing*, vol. 69, no. 4, pp. 293–316, 2006.

[7] M. Sekerli and R. Butera, "An implementation of a simple neuron model in field programmable analog arrays," in *Engineering in Medicine and Biology Society, 2004. IEMBS'04. 26th Annual International Conference of the IEEE*, vol. 2. IEEE, 2004, pp. 4564–4567.

[8] M. F. Simoni, G. S. Cymbalyuk, M. E. Sorensen, R. L. Calabrese, and S. P. DeWeerth, "A multiconductance silicon neuron with biologically matched dynamics," *Biomedical Engineering, IEEE Transactions on*, vol. 51, no. 2, pp. 342–354, 2004.

[9] R. Marston, "Understanding and using OTA OP-AMP ICs," *Nults & Volts Magazine*, pp. 70–74, May 2003.